Nano Research
2024, 17(9): 8495–8503

ISSN 1998-0124 CN 11-5974/O4
https://doi.org/10.1007/s12274-024-6787-y

Research Article

Fluorescent carbon dots synthesized in solid phase and air for application in LEDs

Wei-Jie Zheng, Zhao-Nan Sun, Yi-Ming Wang, and Huan-Ming Xiong (✉)

Department of Chemistry and Shanghai Key Laboratory of Molecular Catalysis and Innovative Materials, Fudan University, Shanghai 200438, China

Received: 12 April 2024 / **Revised:** 17 May 2024 / **Accepted:** 26 May 2024

ABSTRACT

Carbon dots (CDs) have been widely adopted as optical materials because of their excellent luminescent properties. However, most of the reported synthetic methods are conducted in solvents, especially hydrothermal/solvothermal reactions, leading to intractable problems such as toxic and flammable solvents, complex and inseparable by-products, and dangerously high pressures and temperatures. Solid-phase synthesis of CDs in air is an effective solution to overcome the above issues, but solid reactions always result in uncontrolled growth and agglomeration of nanoparticles. In this study, some inorganic salts are selected as catalysts for synthesizing CDs in solid states and air, which also play as dispersants to hinder CDs aggregation. In the meantime, some aromatic derivatives containing hydroxyl and amino groups are chosen as carbon sources, ground with the optimized catalyst, and then heated together in air. The production yields are affected by the reaction time and reactant ratio, while the graphitization degrees of the CDs are determined by the reaction temperature. The I_G/I_D value of their Raman spectra increases from 0.59 to 0.85, and the particle size decreases from 2.5 to 1.4 nm when the synthesis temperature is increased from 200 to 280 °C. The as-prepared CDs show emission peaks ranging from 366 to 606 nm, with the photoluminescence (PL) quantum yield up to 53%. Their emission color variation mainly results from different carbon sources, which can be ascribed to the differences in the element composition, functional groups, and graphitic nitrogen content of these CDs. By dispersing CDs of different concentrations into polyvinyl alcohol (PVA) and combining them with blue LEDs, cold, standard, and warm white light emitting devices (WLEDs) are prepared, with a color rendering index (CRI) up to 84. Since the as-prepared CDs have antioxidant ability at high temperature, the as-prepared WLEDs have long lifespans, remaining the effective white luminescence after 72 h continuous work.

KEYWORDS

carbon dot, solid-phase synthesis, white LED, photoluminescence, inorganic salt catalysis

1 Introduction

Carbon dots (CDs) is a new class of multifunctional carbon material, which are nearly spherical nanoparticles with good dispersion in many solvents, composed of graphitized carbon nuclei, rich functional groups, and cross-linked polymer networks [1–4]. In general, CDs have colorful photoluminescence (PL) properties with widespread applications such as biological imaging, fingerprint recognition, and optical devices [5–10].

CDs are typically synthesized by a bottom-up strategy, wherein small molecules undergo polymerization, crosslinking, and carbonization processes [11–14]. Such a strategy offers various candidates for CDs syntheses, allowing for the modulation of CDs luminescent properties by altering the carbon sources and reaction conditions [15–17]. However, many carbon sources require organic solvents for dispersion and high-pressure autoclaves for synthesis. These conditions not only result in solvent wastage and environmental pollution but also lead to complex purification because solvents always involve in the reactions to produce various by-products [18, 19]. More importantly, safety concerns associated with high pressure reactions make the hydro/solvothermal routes unsuitable for industrial production of CDs. Consequently, recent research about CDs syntheses has been focused on developing green, safe, and large-scale synthetic routes [20–23].

Solid phase synthesis is an effective way to solve the above problems. New methods of heating solid inorganic salts and carbon sources together in autoclaves have been reported in the past several years. Liu et al. [24] found that $AlCl_3 \cdot 6H_2O$ assisted the polymerization of o-phenylenediamine (OPD), and the intermediate polymer was further carbonized under high temperature and pressure to obtain CDs with emission at 590 nm. The authors demonstrated that the salts help produce intermediates with larger conjugated structures before carbonization, which is important to realize red PL emission. Ding et al. [25] used KCl as the catalyst to synthesize full-color emissive CDs from a single carbon source OPD in autoclaves. The authors declared that the fluorescence of their CDs was associated with the degree of graphitization and the ratio of graphitic nitrogen, which could be modified by adjusting the reaction temperature and time. Nevertheless, the above methods still required high-pressure environment within the autoclaves, and more catalysts pairing with different carbon sources were not screened yet. Lately, Niu et al. [26] used SBA-15 as both templates and catalysts, embedding various carbon sources into the channels of SBA-15 to produce diverse fluorescent CDs successfully through pyrolysis in air. By

Address correspondence to hmxiong@fudan.edu.cn

far, much research has revealed that the fluorescence properties of CDs are determined by their composition and surface states which can be changed by switching carbon sources, rather than controlling the particle sizes [26–29].

In this work, a series of carbon sources and several inorganic salts were ground in couples and heated in air to produce fluorescent CDs. Among them, $ZnSO_4$ was chosen as the optimal catalyst, which assisted the pyrolysis of different carbon sources to prepare CDs with tunable PL emission. Both the production yield and quantum yield (QY) of these CDs are considerable, and their emission peaks can be adjusted from 366 to 606 nm owing to different composition and surface states. This method only employs a small amount of ethanol for dissolving CDs, and the ethanol as well as $ZnSO_4$ can be recycled for the next preparation. Thus, both the synthesis cost and the discharged waste are suppressed significantly. The as-prepared CDs exhibit remarkable stability under ambient conditions and can be employed to fabricate long-lasting cold, standard, and warm white light emitting devices (WLEDs).

2 Experimental section

2.1 Materials

Resorcinol, o-phenylenediamine, o-aminophenol, and various carbon sources, inorganic salts such as $ZnSO_4$, and polyvinyl alcohol (PVA, M_W = 88,000) were purchased from Sinopharm Chemical Reagent Co., Ltd. (China). Absolute ethanol was purchased from Shanghai Titan Technology Co., Ltd. (China). Blue LED chips were purchased from Advanced Optoelectronic Technology Co., Ltd. (China). All reagents were used directly without purification.

2.2 Characterization

Field emission transmission electron microscopy (TEM) images were taken by a Tecnai G2 F20 S-Twin electron microscope (FEI, USA) operating at 200 kV. The Raman spectra were obtained using a Horiba-800 Raman spectrometer (HORIBA Jobin Yvon, France) at an excitation wavelength of 785 nm. X-ray diffraction (XRD) patterns were recorded on a Bruker D2 PHASER diffractometer (Bruker, Germany). FTIR spectra were measured on a Nicolet iS10 spectrometer (ThermoFisher, USA). X-ray photoelectron spectroscopy (XPS) data were collected by a PHI 5000C & PHI 5300 spectrometer (PHI, USA). UV–Vis absorption spectra were scanned by a UV-2802 PC spectrophotometer (UNICO, USA). The fluorescence spectra and the absolute fluorescence quantum yield were measured on a Horiba Jobin Yvon FluoroMax-4 spectrofluorometer (HORIBA Jobin Yvon, France) with an F-3018 integrating sphere. The thermogravimetric analysis (TGA) was carried out with NETZSCH TG 209 F1 Libra (NETZSCH, Gemany) from 30 to 800 °C with a heating rate of 10 °C/min.

2.3 Syntheses of CDs

2.3.1 Reaction combinations of various carbon sources and inorganic salts

1.0 g of carbon source and 1.0 g of inorganic salt were mixed in a mortar and ground for 30 min. The obtained powder was made into a sheet by a tablet press under 20 kPa to prevent the powder from blowing out during heating and then put into a glass beaker. The beaker was coated by a glass sheet and placed in a blast drying oven at 200 °C for 3 h. After cooling down to room temperature, the reaction product was ground into powder for CDs separation. 4 mL of water was added to dissolve $ZnSO_4$ by sonication, and then the mixture was centrifugated to remove the aqueous solution. Afterward, 20 mL of ethanol was added for dissolving CDs by ultrasonication, and then the mixture was centrifuged at 5000 rpm for 6 min to collect the solution. In this way, the sediment was extracted by ethanol repeatedly, and all of the collected solution was dried by rotary evaporation to obtain CDs powder, while the condensed ethanol was collected for recycling. At last, the residual black sediment was regarded as the carbon soot, which could be eliminated by calcination in air.

2.3.2 Regulation of reaction conditions

To optimize the reaction ratio, 1.0 g of OPD was ground with 0, 0.25, 0.5, 1.0, 2.0, and 4.0 g of $ZnSO_4$ and then pressed into tablets for 3 h heating. The temperature was set at 180, 200, 220, 240, 260, and 280 °C to study the reaction using 1.0 g of $ZnSO_4$. For the same reaction ratio, the heating was maintained for 1, 2, 3, 4, and 5 h at 200 °C to investigate the duration effect. All products were separated by the same process as described in Section 2.3.1. The production yield was simply calculated through dividing the mass of the CDs by the mass of the carbon source.

2.3.3 Synthesis of B-, G-, Y-CDs

1.0 g of resorcinol, o-phenylenediamine, and o-aminophenol were mixed with 1.0 g of $ZnSO_4$ respectively and heated at 200 °C for 3 h to produce CDs with blue, green, and yellow fluorescence, which were named as B-, G-, and Y-CDs, respectively.

2.4 Recovery and reuse of $ZnSO_4$

After washing by ethanol and centrifugation, the precipitate was dried in a blast drying oven at 80 °C and then calcined in a tubular furnace at 600 °C for 5 h. The product was the recovered $ZnSO_4$. 1.0 g of OPD was ground with 1.0 g of such recycled $ZnSO_4$ and pressed together for 3 h reaction at 200 °C, followed by extraction with ethanol as described in Section 2.3.1.

2.5 Fabrication of WLEDs

Cold, standard, and warm WLEDs were prepared by coating PVA glue containing OPD-CDs of different concentrations. Firstly, 2.0 g PVA powder was dissolved in 10 mL of water under continuous magnetic stirring. Then, 0.2, 0.3, and 0.5 g of OPD-CDs were dispersed in 10 mL of ethanol by ultrasound. Afterward, 1.0 mL of 0.02, 0.03, and 0.05 g/mL OPD-CDs ethanol solutions were mixed with 9.0 mL of PVA aqueous solution, and the solutions were dried in a blast drying oven at 80 °C for 30 min. Finally, the obtained PVA glue was coated on a 460 nm of blue LED chip and placed in a constant temperature oven at 60 °C for 2 h curing to prepare the cold, standard, and warm WLEDs.

3 Results and discussion

Scheme 1 illustrates the solid-phase synthesis approach proposed in this research, which produces multicolor fluorescent CDs through the catalyzed pyrolysis of different carbon sources. Many kinds of inorganic salts were tested, and some results are shown in Table S1 in the Electronic Supplementary Material (ESM). It was found that NaCl, KCl, and Na_2SO_4 did not exhibit any catalytic effect, whereas acidic inorganic salts like $ZnCl_2$, $ZnSO_4$, and $NaHSO_4$ exhibit significant catalytic effects. According to the formation mechanism of carbonized polymer dots, the small molecules containing benzene and naphthalene rings firstly polymerize to form polymers and subsequently carbonize into CDs. Hence, the acidic inorganic salts catalyzed the polymerization process on one hand, and on the other hand, prevented the oxidative decomposition of organic molecules at high temperatures in air [19, 30]. Particularly, $ZnCl_2$ and $ZnSO_4$

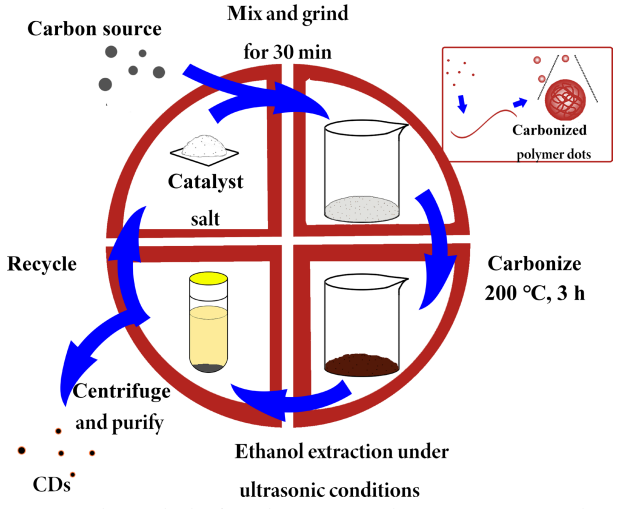

Scheme 1 The method of synthesizing CDs by using inorganic salts as dispersants and catalysts in air.

assisted reactions resulted in higher yields and fluorescence intensities compared to $NaHSO_4$. Because $ZnCl_2$ absorbs moisture easily in grinding, $ZnSO_4$ was chosen as the optimal catalyst, and the following experiments were carried out with $ZnSO_4$.

The yield of CDs was simply calculated by dividing the mass of the CDs by the mass of the carbon source. In general, our CDs are soluble in ethanol but insoluble in water, so they can be washed away from the products by absolute ethanol and then dried into powder form. Before extraction with ethanol, the product had a large amount of $ZnSO_4$ which was removed by water dissolution. However, some CDs are hydrophilic and thus, washing by water will cause loss of CDs. Hence in Table 1, some reactions have high yields even over 50%, while p-phenylenediamine derived CDs are rather few. To verify that the fluorescent products obtained were CDs, the samples were observed under TEM (Fig. S1 in the ESM), and their PL spectra were also measured. Depending on the carbon sources, the emission peak of the obtained CDs varies from 366 to 606 nm (Fig. 1). All samples show their emission wavelengths do not shift along with the excitation light, which means the CDs have good purity. Particularly, the OPD derived CDs exhibit a high PL quantum yield up to 53%.

Subsequently, the OPD involved synthesis was chosen to investigate the effects of reaction conditions on the yields and PL intensities of the OPD-CDs. These conditions include the feed ratios between OPD and $ZnSO_4$, the reaction temperatures, and the reaction time. In Fig. 2(a), no formation of CDs is observed without $ZnSO_4$ involvement, because OPD will be oxidized and decomposed at the high temperature. The TGA curves of OPD in Fig. S2(a) in the ESM shows OPD decomposition begins at 100 °C and completes at 180 °C. After addition of $ZnSO_4$, OPD molecules are polymerized and carbonized, so its decomposition at high temperatures is prevented [31]. As the amount of $ZnSO_4$ increases, the yield of CDs increases gradually. But when $ZnSO_4$ is excess, the complete separation of CDs from the product became difficult.

The adjustment of the reaction temperature was based on the TGA result that OPD completes decomposition at 180 °C. The reaction temperature was set above 180 °C to eliminate any OPD residues, and the feed ratio was set as 1:1. As shown in Fig. 2(b), with the increase in reaction temperature, the yield gradually decreases. Such a decrease at high temperatures can be attributed to several reasons. One is the CDs aggregation, forming large particles that are insoluble in ethanol. Another is the formation of soot, which will be blown away from the beaker. The last is the decomposition of CDs, which was discovered recently [32]. The TGA curve (Fig. S2(b) in the ESM) of CDs synthesized at 200 °C indicates that OPD-CDs maintain thermal stability below 220 °C, but start to lose weight upon heating above 227 °C. As the temperature increases gradually to 700 °C, the weight loss of CDs continues until they are totally decomposed in air. Figure 2(c) reveals the relationship between the reaction time and the yield. The maximum yield is obtained when the reaction time is 2.5–3 h. The extension of reaction time cannot improve the yield,

Table 1 The yield and PLQY of CDs prepared by changing carbon sources.

Carbon source	Emission peak	Quantum yield	Yield
m-Aminophenol	366 nm	18%	14%
1,5-Dihydroxynaphthalene	463 nm	34%	35%
Resorcinol	530 nm	31%	56%
o-Phenylenediamine	548 nm	53%	34%
o-Aminophenol	567 nm	26%	43%
p-Phenylenediamine	606 nm	7%	2.5%

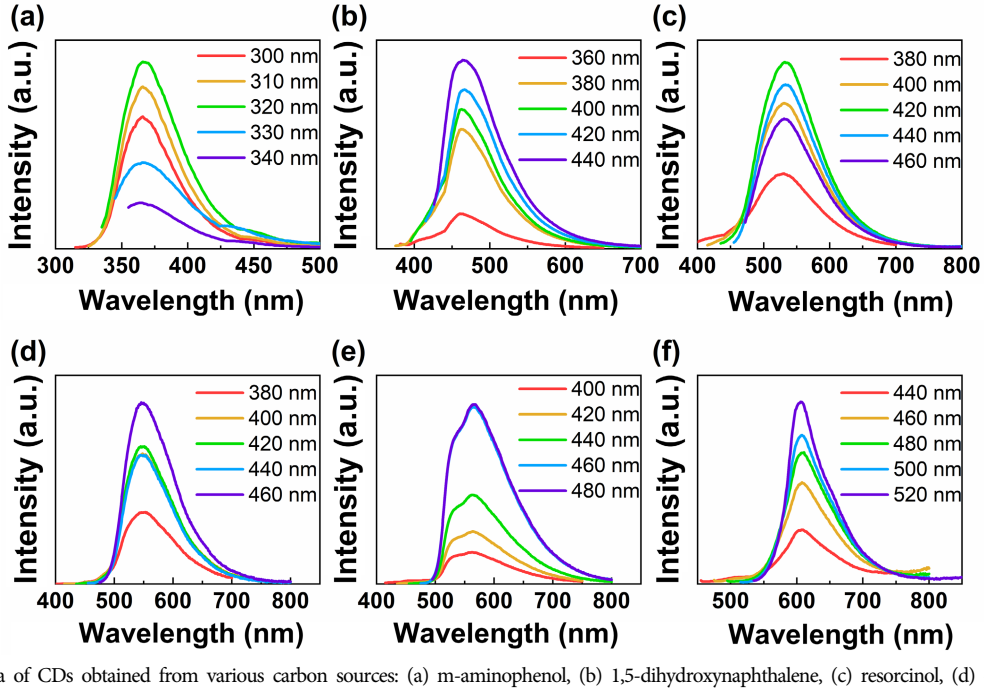

Figure 1 PL spectra of CDs obtained from various carbon sources: (a) m-aminophenol, (b) 1,5-dihydroxynaphthalene, (c) resorcinol, (d) o-phenylenediamine, (e) o-aminophenol, and (f) p-phenylenediamine.

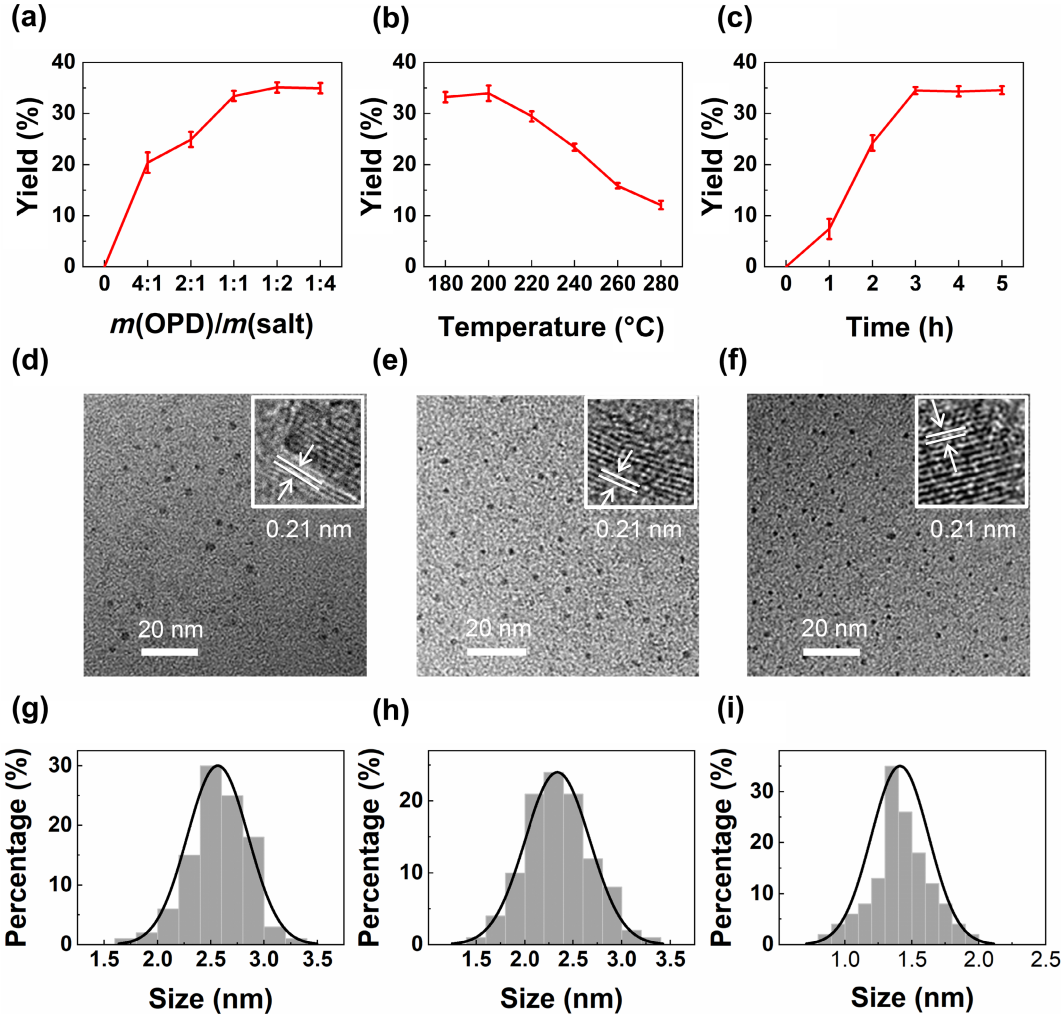

Figure 2 Relationship between the production yield and (a) the feed ratio of OPD/$ZnSO_4$ at 200 °C for 3 h, (b) the reaction temperature at 1:1 ratio for 3 h, and (c) reaction time at 1:1 ratio and 200 °C. TEM images of CDs synthesized at (d) 200, (e) 240, and (f) 280 °C. Particle size distribution of CDs synthesized at (g) 200, (h) 240, and (i) 280 °C.

indicating that the carbon source has been exhausted and transformed. The TEM images of CDs obtained at different temperatures and the corresponding particle size distribution are illustrated in Figs. 2(d)–2(i). These OPD-CDs are spherical nanoparticles with good dispersion and no obvious aggregation. It is interesting that the temperature increase induces CDs diameter decrease, from ca. 2.5 nm to ca. 1.4 nm. But their carbon cores as shown in the inset HRTEM images do not change significantly, with the typical graphitization (100) lattice spacing of 0.21 nm [33]. This phenomenon is ascribed to the gradual carbonization of the polymer chain wrapped on the surface of the CDs, which leads to the reduction of the particle sizes [34].

Under different reaction conditions, the PL emission peak of the obtained OPD-CDs is consistent (Fig. 3(a)), and the maximum emission wavelength is stable at 548 nm. However, the reaction temperature has a significant effect on the PL intensities of CDs, and heating at high temperature such as 280 °C will weaken the samples' fluorescence. This result indicates that the luminescent centers probably locate at the CDs surfaces but not the carbon cores. To verify this hypothesis, Raman spectroscopy and XRD analyses were performed for the OPD-CDs synthesized at different temperatures. In the Raman spectra (Fig. 3(b)), all samples show two peaks at 1355 and 1563 cm^{-1}, corresponding to the disordered carbon structure and the graphitic carbon structure, respectively [35]. As the synthesis temperature increased, the peak area intensity ratio (I_G/I_D) of the CDs gradually increased from 0.59 (obtained at 200 °C) to 0.85 (obtained at 280 °C), reflecting an enhancement in the degree of graphitization of the CDs [36]. The XRD patterns (Fig. 3(c)) show that with the increase of the synthesis temperature, the characteristic peak of graphitization is gradually obvious, and the intensity of the peak increases accordingly, which also verifies the increase of graphitization of the CDs [37].

To explore the influence of carbon sources on the fluorescence properties of CDs, three kinds of CDs made from resorcinol, o-phenylenediamine, and o-aminophenol were selected for comparison. They are named as B-CDs, G-CDs, and Y-CDs, respectively according to their luminescence colors (Figs. 3(d)–3(f)). In general, the different fluorescence colors of CDs with similar particles are ascribed to the differences between their surface states and the heteroatom doping [38, 39]. The UV–Vis absorption spectra of the three samples display strong π–π absorption peaks in the UV region (< 300 nm), which are attributed to the large conjugated structure of CDs [40]. Different from B-CDs, G-CDs and Y-CDs display obvious n–π transition absorption at longer wavelengths, owing to the N species in the material [41]. The absorption peaks of B-CDs and Y-CDs at about 350 nm are attributed to the n–π transition of O species. Since resorcin has more oxygen content and can derive more O species than O-aminophenol, B-CDs exhibit a wider absorption peak in the 290–350 nm region [42].

The FT-IR spectra of these CDs (Fig. 4) show wide and strong bands near 3400 cm^{-1}, indicating that there are plenty of O–H and N–H bonds in CDs. The infrared bands of CDs are usually wider and gentler than those of raw materials, because there are complex superposition of surface functional groups in CDs [43]. At

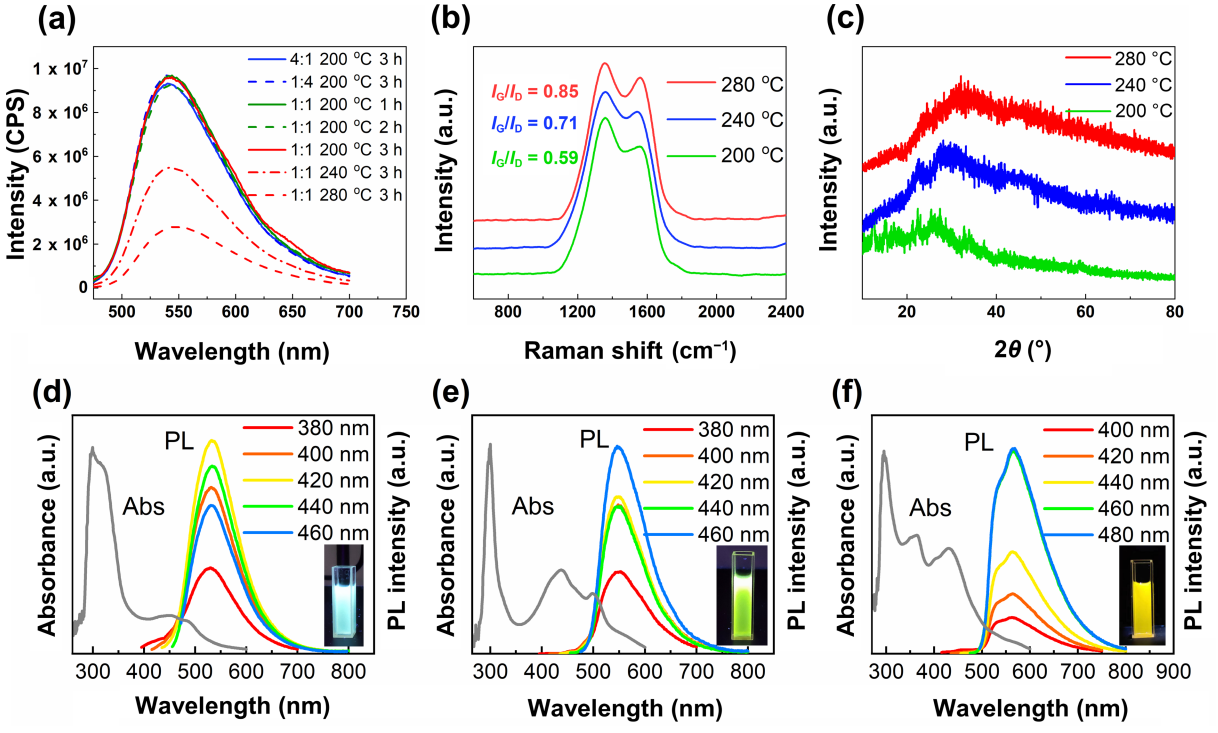

Figure 3 (a) PL spectra (excited at 420 nm) of OPD-CDs (0.1 mg/mL) synthesized under different reaction conditions. (b) Raman spectra and (c) XRD patterns of OPD-CDs obtained at the different temperatures. UV–Vis absorption spectra and PL spectra of (d) B-CDs, (e) G-CDs, and (f) Y-CDs.

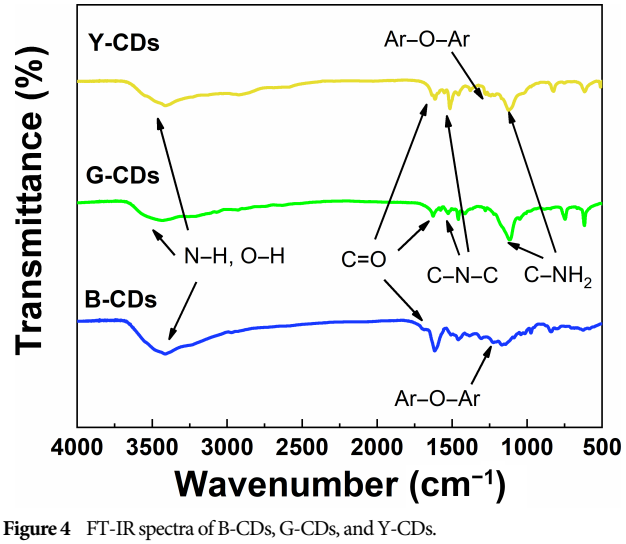

Figure 4 FT-IR spectra of B-CDs, G-CDs, and Y-CDs.

1225 cm^{-1}, B-CDs and Y-CDs exhibit characteristic peaks corresponding to the asymmetric stretching vibrations of Ar–O–Ar in the aryl ether structures. The peak intensity of Y-CDs at 1225 cm^{-1} is smaller than that of B-CDs, while G-CDs has no such peak, which reveals that B-CDs and Y-CDs are probably formed by polymerization through dehydration between hydroxyl groups [44, 45]. As for G-CDs, the o-phenylenediamine molecules usually polymerize through a phenazine route [42]. The three CDs show obvious C=O stretching vibration peaks at 1630 cm^{-1}, which may be ascribed to oxidation by air. The peaks of G-CDs and Y-CDs at 1521 cm^{-1} prove that the polymerization of OPD and o-aminophenol causes N element to enter the aromatic ring skeleton, and this characteristic peak is the stretching vibration of C=N in the aromatic ring skeleton [46]. The strong peaks at 1116 cm^{-1} of G-CDs and Y-CDs correspond to the in-plane bending vibrations of primary amine N–H bonds, suggesting that the amino groups from the raw material have been carried by the CDs. The peak strength of the N–H bond of G-CDs is significantly greater than that of Y-CDs, which is consistent with the polymerization process from o-phenylenediamine to phenazine intermediates, resulting in more amino groups on the G-CDs surfaces.

The full XPS spectra (Fig. 5(a)) reflect the effects of different carbon sources on the heteroatoms in CDs. G-CDs and Y-CDs show peaks at 283, 403, and 534 eV corresponding to the energy spectra of C 1s, N 1s, and O 1s, respectively [47]. For B-CDs, peaks at 284 and 532 eV correspond to the energy spectra of C 1s and O 1s. It is clear that N species originated from the precursors, while O species derived from oxidation at high temperatures. Since o-phenylenediamine has more N content than o-aminophenol, the N 1s peak of G-CDs shows a larger area than that of Y-CDs. Detailed spectrum analyses of these CDs reveal that the N 1s peaks for G-CDs and Y-CDs (Figs. 5(b) and 5(c)) can be divided into pyridinic nitrogen (398.2 eV), amino nitrogen (399.5 eV), and graphitic nitrogen (400.7 eV) [48]. It is evident that Y-CDs have a higher proportion of graphitic nitrogen compared to G-CDs, which may be the reason for the fluorescence redshift. The C 1s peak of G-CDs and Y-CDs can be deconvoluted into four peaks, corresponding to C–C/C=C (284.5 eV), C–N (285.5 eV), C–O (286.4 eV), and C=O (288.0 eV), verifying the presence of functional groups such as amino, carboxyl, and hydroxyl on the CDs [49]. The C 1s peak for B-CDs can be deconvoluted into three peaks: C–C/C=C (284.5 eV), C–O (286.1 eV), and C=O (287.9 eV) (Figs. 5(d)–5(f)). Since there is no N element in the raw material for B-CDs, there is no C–N peak in the C 1s of B-CDs. The O 1s peaks (Figs. 5(g)–5(i)) of these CDs are divided into two components, corresponding to C–O (532.3 eV for B-CDs and G-CDs and 532.5 eV for Y-CDs) and C=O (533.6 eV). The appearance of the C=O peak is due to the oxidation of the surface hydroxyl groups [50]. The element species and the corresponding proportions are presented in Table S2 in the ESM.

After reactions, $ZnSO_4$ was washed away from the product by water. The aqueous solution was recrystallized and then calcined at 600 °C for 5 h. The recycled $ZnSO_4$ was compared with the new commercial $ZnSO_4$ by XRD measurement. Their patterns are also the same in Fig. 6(a), confirming that the recycling is successful.

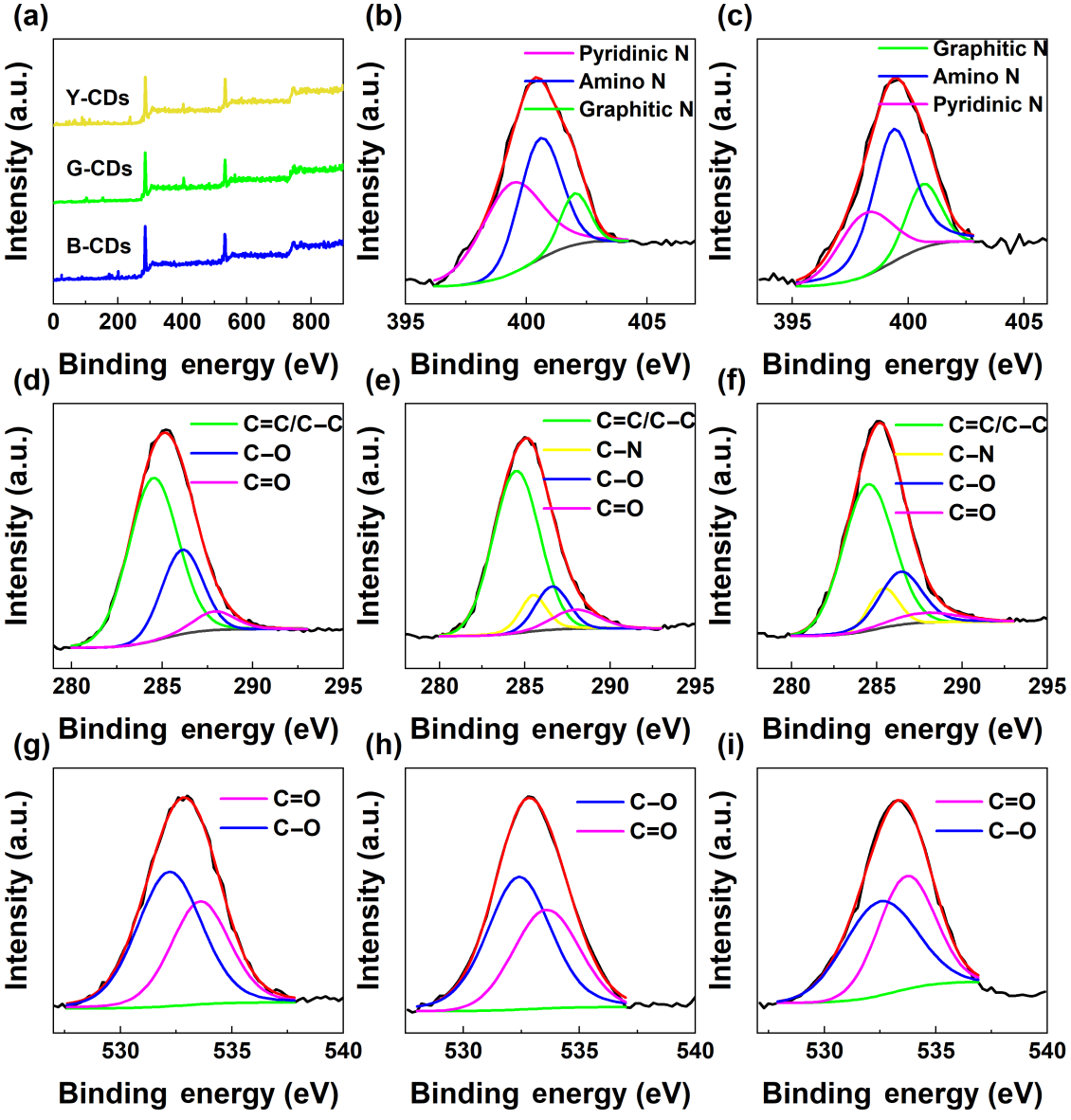

Figure 5 (a) XPS full spectra of B-CDs, G-CDs, and Y-CDs. XPS N 1s spectra of (b) G-CDs and (c) Y-CDs. XPS C 1s spectra of (d) B-CDs, (e) G-CDs, and (f) Y-CDs. XPS O 1s spectra of (g) B-CDs, (h) G-CDs, and (i) Y-CDs.

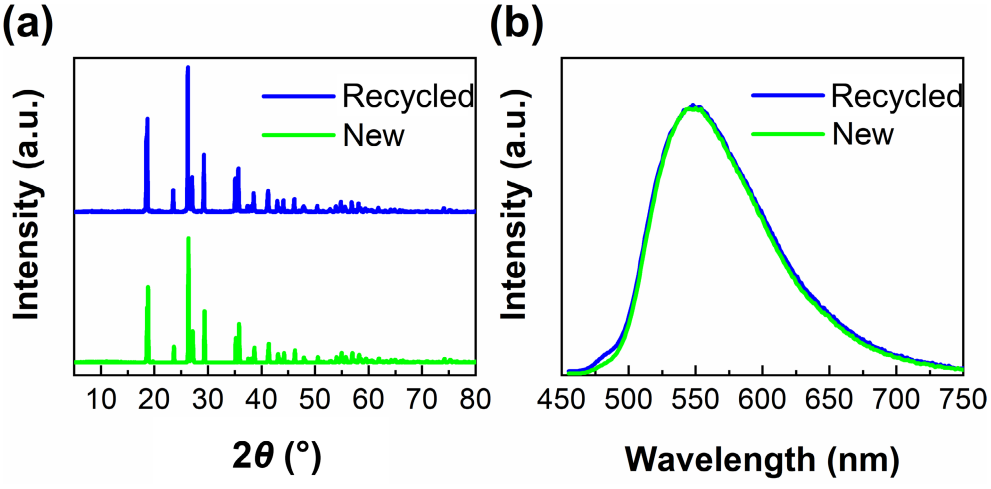

Figure 6 (a) XRD spectra of recycled and new $ZnSO_4$. (b) PL spectra of OPD-CDs synthesized by recycled and new $ZnSO_4$.

The recycled $ZnSO_4$ was also used to synthesize OPD-CDs (Fig. 6(b)), which exhibit the same PL spectra with those synthesized using the commercial $ZnSO_4$. The mass loss of $ZnSO_4$ after the reaction is very small, and thus $ZnSO_4$ can be recycled for repeated syntheses. In addition, the ethanol as the solvent for extracting CDs from the products can also be recycled by rotary evaporation and further purification. Therefore, our method meets the requirement of green chemistry.

Many photoluminescent materials have been tested in the LEDs, but failed in long time working, because their photostability

at high temperatures and against oxidation are insufficient. Our CDs are produced in air at high temperature, so they have good thermal stability against oxidation naturally [6, 36]. By changing the mass concentrations of OPD-CDs in PVA to adjust the luminescence intensity of the substrate, cold, standard, and warm-WLEDs were obtained (Fig. 7). 2 mg/mL OPD-CDs in a 20 wt.% PVA solution were dried for preparing a cold WLED with a color temperature of 7140 K, a color coordinate of (0.3093, 0.2935), and a color rendering index (CRI) of 79.6 (Fig. 7(a)). When the concentration of OPD-CDs was increased to 3 mg/mL, the as-prepared LED shows a standard white light with a color temperature of 5378 K, a color coordinate of (0.3347, 0.3309), and a CRI of 82.7 (Fig. 7(b)). Further adding the OPD-CDs to a concentration of 5 mg/mL resulted in a warm WLED with a color temperature of 4485 K, a color coordinate of (0.3586, 0.3490), and a CRI of 84.2 (Fig. 7(c)). All of the above WLEDs possess good stability, which can maintain their effective luminescence spectra and intensities for over 72 h (Fig. S3 in the ESM).

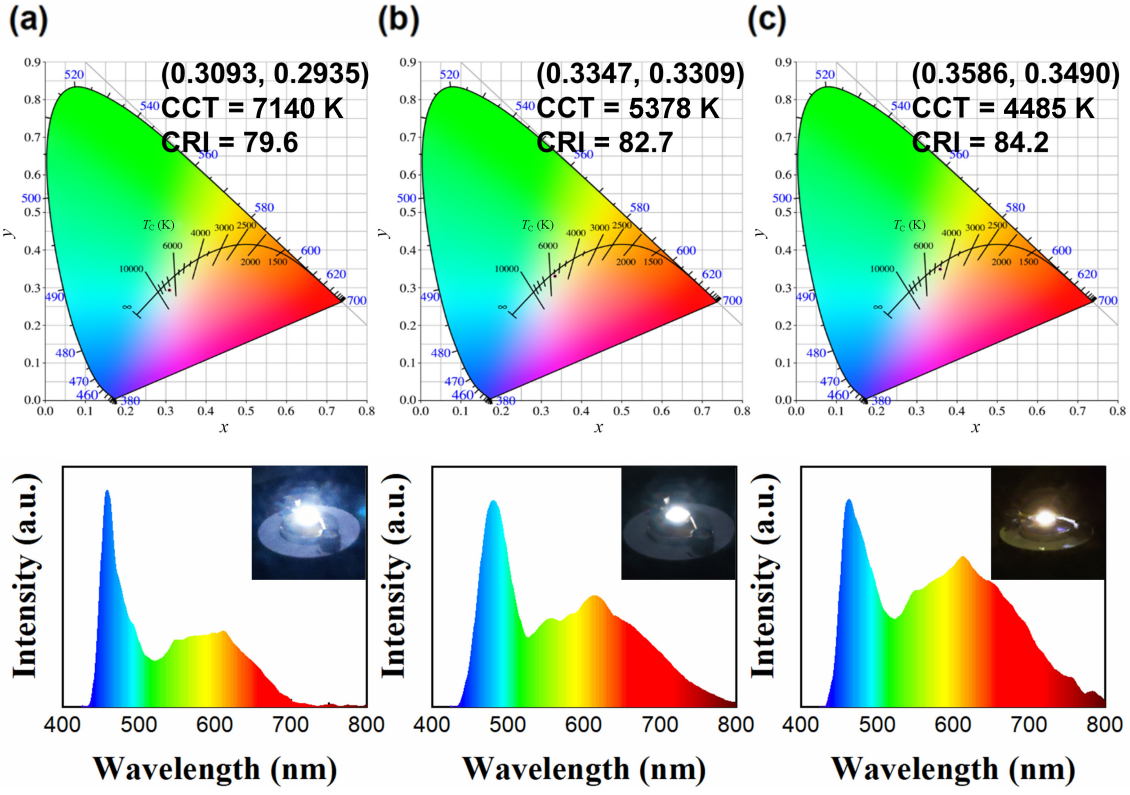

Figure 7 The CIE color coordinates and emission light spectra of (a) cold, (b) standard, and (c) warm WLEDs prepared by different concentrations of OPD-CDs.

4 Conclusions

We invented a method for the solid-phase synthesis of full-color luminescent CDs in air. In this method, inorganic salts act as the catalysts and the dispersants, catalyzing the carbon sources polymerization and carbonization at high temperatures and preventing the direct thermal decomposition of the carbon source in air and the aggregation of the carbonized polymer dots. All conditions for such syntheses have been investigated with detailed characterization. The results indicate that carbon sources are the dominant factors that determine the compositions, structures, and properties of the obtained CDs, especially their fluorescence. Our synthetic method has many advantages, including low cost, environmental friendliness, simple operation, short time, and large scale. We believe that by screening more carbon sources and optimizing the catalysts, more CDs with excellent properties for practical applications will be found through this way in the future.

Acknowledgements

This work was financially supported by the National Natural Science Foundation of China (No. 21975048) and the Shanghai Science and Technology Committee (No. 19DZ2270100).

Electronic Supplementary Material: Supplementary material (results of different combinations of inorganic salts and carbon sources, elements and compositions of different CDs obtained by XPS measurement, TEM images of CDs obtained from various carbon sources, TGA curves of OPD and OPD-CDs, and PL intensity change of WLEDs during long working time) is available in the online version of this article at https://doi.org/10.1007/s12274-024-6787-y.

References

[1] Yan, Y. B.; Gong, J.; Chen, J.; Zeng, Z. P.; Huang, W.; Pu, K. Y.; Liu, J. Y.; Chen, P. Recent advances on graphene quantum dots: From chemistry and physics to applications. *Adv. Mater.* **2019**, *31*, 1808283.

[2] Lim, S. Y.; Shen, W.; Gao, Z. Q. Carbon quantum dots and their applications. *Chem. Soc. Rev.* **2015**, *44*, 362–381.

[3] Liu, J. J.; Li, R.; Yang, B. Carbon dots: A new type of carbon-based nanomaterial with wide applications. *ACS Cent. Sci.* **2020**, *6*, 2179–2195.

[4] Bartelmess, J.; Quinn, S. J.; Giordani, S. Carbon nanomaterials: Multi-functional agents for biomedical fluorescence and Raman imaging. *Chem. Soc. Rev.* **2015**, *44*, 4672–4698.

[5] Liu, J.; Kong, T. Y.; Xiong, H. M. Mulberry-leaves-derived red-emissive carbon dots for feeding silkworms to produce brightly fluorescent silk. *Adv. Mater.* **2022**, *34*, 2200152.

[6] Yuan, F. L.; He, P.; Xi, Z. F.; Li, X. H.; Li, Y. C.; Zhong, H. Z.; Fan, L. Z.; Yang, S. H. Highly efficient and stable white LEDs based on pure red narrow bandwidth emission triangular carbon quantum dots for wide-color gamut backlight displays. *Nano Res.* **2019**, *12*, 1669–1674.

[7] Jiang, L.; Cai, H.; Zhou, W. W.; Li, Z. J.; Zhang, L.; Bi, H. RNA-targeting carbon dots for live-cell imaging of granule dynamics. *Adv. Mater.* **2023**, *35*, 2210776.
[8] Li, P. F.; Sun, L.; Xue, S. S.; Qu, D.; An, L.; Wang, X. Y.; Sun, Z. C. Recent advances of carbon dots as new antimicrobial agents. *SmartMat* **2022**, *3*, 226–248.
[9] Zhang, Y. Q.; Liu, K. X.; Yu, J. K.; Chen, H. F.; Fu, R.; Zhu, S. Q.; Chen, Z. Q.; Wang, S. P.; Lu, S. Y. Single stain hyperspectral imaging for accurate fungal pathogens identification and quantification. *Nano Res.* **2022**, *15*, 6399–6406.
[10] Wang, Z. F.; Yuan, F. L.; Li, X. H.; Li, Y. C.; Zhong, H. Z.; Fan, L. Z.; Yang, S. H. 53% efficient red emissive carbon quantum dots for high color rendering and stable warm white-light-emitting diodes. *Adv. Mater.* **2017**, *29*, 1702910.
[11] Ding, H. Z.; Xu, J. H.; Jiang, L.; Dong, C.; Meng, Q.; ur Rehman, S.; Wang, J. F.; Ge, Z. S.; Osipov, V. Y.; Bi, H. Fluorine-defects induced solid-state red emission of carbon dots with an excellent thermosensitivity. *Chin. Chem. Lett.* **2021**, *32*, 3646–3651.
[12] Yang, F.; LeCroy, G. E.; Wang, P.; Liang, W. X.; Chen, J. J.; Fernando, K. A. S.; Bunker, C. E.; Qian, H. J.; Sun, Y. P. Functionalization of carbon nanoparticles and defunctionalization—toward structural and mechanistic elucidation of carbon "quantum" dots. *J. Phys. Chem. C* **2016**, *120*, 25604–25611.
[13] Wang, B. Y.; Lu, S. Y. The light of carbon dots: From mechanism to applications. *Matter.* **2022**, *5*, 110–149.
[14] Tao, S. Y.; Zhou, C. J.; Kang, C. Y.; Zhu, S. J.; Feng, T. L.; Zhang, S. T.; Ding, Z. Y.; Zheng, C. Y.; Xia, C. L.; Yang, B. Confined-domain crosslink-enhanced emission effect in carbonized polymer dots. *Light Sci. Appl.* **2022**, *11*, 56.
[15] Đorđević, L.; Arcudi, F.; D'Urso, A.; Cacioppo, M.; Micali, N.; Bürgi, T.; Purrello, R.; Prato, M. Design principles of chiral carbon nanodots help convey chirality from molecular to nanoscale level. *Nat. Commun.* **2018**, *9*, 3442.
[16] Ru, Y.; Ai, L.; Jia, T. T.; Liu, X. J.; Lu, S. Y.; Tang, Z. Y.; Yang, B. Recent advances in chiral carbonized polymer dots: From synthesis and properties to applications. *Nano Today* **2020**, *34*, 100953.
[17] Ding, H.; Zhou, X. X.; Wei, J. S.; Li, X. B.; Qin, B. T.; Chen, X. B.; Xiong, H. M. Carbon dots with red/near-infrared emissions and their intrinsic merits for biomedical applications. *Carbon.* **2020**, *167*, 322–344.
[18] Ding, H.; Yu, S. B.; Wei, J. S.; Xiong, H. M. Full-color light-emitting carbon dots with a surface-state-controlled luminescence mechanism. *ACS Nano* **2016**, *10*, 484–491.
[19] Liu, J. J.; Li, D. W.; Zhang, K.; Yang, M. X.; Sun, H. C.; Yang, B. One-step hydrothermal synthesis of nitrogen-doped conjugated carbonized polymer dots with 31% efficient red emission for *in vivo* imaging. *Small* **2018**, *14*, 1703919.
[20] Jiang, K.; Wang, Y. H.; Gao, X. L.; Cai, C. Z.; Lin, H. W. Facile, quick, and gram-scale synthesis of ultralong-lifetime room-temperature-phosphorescent carbon dots by microwave irradiation. *Angew. Chem., Int. Ed.* **2018**, *57*, 6216–6220.
[21] Ji, C. Y.; Han, Q. R.; Zhou, Y. Q.; Wu, J. J.; Shi, W. Q.; Gao, L. P.; Leblanc, R. M.; Peng, Z. L. Phenylenediamine-derived near infrared carbon dots: The kilogram-scale preparation, formation process, photoluminescence tuning mechanism and application as red phosphors. *Carbon* **2022**, *192*, 198–208.
[22] Liu, X. X.; Yang, C. L.; Zheng, B. Z.; Dai, J. Y.; Yan, L.; Zhuang, Z. J.; Du, J.; Guo, Y.; Xiao, D. Green anhydrous synthesis of hydrophilic carbon dots on large-scale and their application for broad fluorescent pH sensing. *Sens. Actuat. B Chem.* **2018**, *255*, 572–579.
[23] Xu, W. J.; Zeng, F. H.; Han, Q. R.; Peng, Z. L. Recent advancements of solid-state emissive carbon dots: A review. *Coord. Chem. Rev.* **2024**, *498*, 215469.
[24] Liu, K. K.; Song, S. Y.; Sui, L. Z.; Wu, S. X.; Jing, P. T.; Wang, R. Q.; Li, Q. Y.; Wu, G. R.; Zhang, Z. Z.; Yuan, K. J. et al. Efficient red/near-infrared-emissive carbon nanodots with multiphoton excited upconversion fluorescence. *Adv. Sci.* **2019**, *6*, 1900766.
[25] Ding, H.; Zhou, X. X.; Zhang, Z. H.; Zhao, Y. P.; Wei, J. S.; Xiong, H. M. Large scale synthesis of full-color emissive carbon dots from a single carbon source by a solvent-free method. *Nano Res.* **2022**, *15*, 3548–3555.
[26] Niu, X. Q.; Zheng, W. J.; Song, T. B.; Huang, Z. H.; Yang, C. L.; Zhang, L. M.; Li, W.; Xiong, H. M. Pyrolysis of single carbon sources in SBA-15: A recyclable solid phase synthesis to obtain uniform carbon dots with tunable luminescence. *Chin. Chem. Lett.* **2023**, *34*, 107560.
[27] Xu, J. H.; Liang, Q. J.; Li, Z. J.; Osipov, V. Y.; Lin, Y. J.; Ge, B. H.; Xu, Q.; Zhu, J. F.; Bi, H. Rational synthesis of solid-state ultraviolet B emitting carbon dots via acetic acid-promoted fractions of sp^3 bonding strategy. *Adv. Mater.* **2022**, *34*, 2200011.
[28] Miao, X.; Qu, D.; Yang, D. X.; Nie, B.; Zhao, Y. K.; Fan, H. Y.; Sun, Z. C. Synthesis of carbon dots with multiple color emission by controlled graphitization and surface functionalization. *Adv. Mater.* **2018**, *30*, 1704740.
[29] Lin, C. J.; Zhuang, Y. X.; Li, W. H.; Zhou, T. L.; Xie, R. J. Blue, green, and red full-color ultralong afterglow in nitrogen-doped carbon dots. *Nanoscale* **2019**, *11*, 6584–6590.
[30] Liu, Y. D.; Yu, Y. K.; Yang, F.; Zhu, G. Q.; Yu, K.; Kou, R. H.; Sun, C. J.; Liu, Y. Z.; Xu, J. Y.; Liu, C. et al. Reversible iron oxyfluoride (FeOF)–graphene composites as sustainable cathodes for high energy density lithium batteries. *Small.* **2023**, *19*, 2206947.
[31] Liu, H. X.; Zhong, X.; Pan, Q.; Zhang, Y.; Deng, W. T.; Zou, G. Q.; Hou, H. S.; Ji, X. B. A review of carbon dots in synthesis strategy. *Coord. Chem. Rev.* **2024**, *498*, 215468.
[32] Li, Y.; Liu, C.; Sun, H.; Chen, M. L.; Hou, D. F.; Zheng, Y. W.; Xie, H. J.; Zhou, B.; Lin, X. Formation and band gap tuning mechanism of multicolor emissive carbon dots from *m*-hydroxybenzaldehyde. *Adv. Sci.* **2023**, *10*, 2300543.
[33] Song, S. Y.; Liu, K. K.; Mao, X.; Cao, Q.; Li, N.; Zhao, W. B.; Wang, Y.; Liang, Y. C.; Zang, J. H.; Li, X. et al. Colorful triplet excitons in carbon nanodots for time delay lighting. *Adv. Mater.* **2023**, *35*, 2212286.
[34] Wang, B. Y.; Song, H. Q.; Tang, Z. Y.; Yang, B.; Lu, S. Y. Ethanol-derived white emissive carbon dots: The formation process investigation and multi-color/white LEDs preparation. *Nano Res.* **2022**, *15*, 942–949.
[35] Ding, H.; Zhao, R.; Zhang, Z. H.; Yang, J. J.; Wang, Z.; Xiao, L. L.; Li, X. H.; He, X. J.; Xiong, H. M. Kilogram-scale synthesis of carbon dots with high-efficiency full-color solid-state fluorescence using an aggregation-induced emission strategy. *Chem. Eng. J.* **2023**, *476*, 146405.
[36] Xu, W. J.; Han, Q. R.; Ji, C. Y.; Zeng, F. H.; Zhang, X. S.; Deng, J. W.; Shi, C. S.; Peng, Z. L. Solid-state, hectogram-scale preparation of red carbon dots as phosphor for energy-transfer-induced high-quality white LEDs with CRI of 97. *Small* **2023**, *19*, 2304123
[37] Qu, D.; Zheng, M.; Li, J.; Xie, Z. G.; Sun, Z. C. Tailoring color emissions from N-doped graphene quantum dots for bioimaging applications. *Light Sci. Appl.* **2015**, *4*, e364.
[38] Bao, L.; Liu, C.; Zhang, Z. L.; Pang, D. W. Photoluminescence-tunable carbon nanodots: Surface-state energy-gap tuning. *Adv. Mater.* **2015**, *27*, 1663–1667.
[39] Jiang, K.; Sun, S.; Zhang, L.; Lu, Y.; Wu, A. G.; Cai, C. Z.; Lin, H. W. Red, green, and blue luminescence by carbon dots: Full-color emission tuning and multicolor cellular imaging. *Angew. Chem., Int. Ed.* **2015**, *54*, 5360–5363.
[40] Niu, X. Q.; Song, T. B.; Xiong, H. M. Large scale synthesis of red emissive carbon dots powder by solid state reaction for fingerprint identification. *Chin. Chem. Lett.* **2021**, *32*, 1953–1956.
[41] Jiang, K.; Gao, X. L.; Feng, X. Y.; Wang, Y. H.; Li, Z. J.; Lin, H. W. Carbon dots with dual-emissive, robust, and aggregation-induced room-temperature phosphorescence characteristics. *Angew. Chem., Int. Ed.* **2020**, *59*, 1263–1269.
[42] Li, P. F.; Xue, S. S.; Sun, L.; Zong, X. P.; An, L.; Qu, D.; Wang, X. Y.; Sun, Z. C. Formation and fluorescent mechanism of red emissive carbon dots from *o*-phenylenediamine and catechol system. *Light Sci. Appl.* **2022**, *11*, 298.
[43] Sun, H. C.; Xia, P. F.; Shao, H. B.; Zhang, R.; Lu, C. G.; Xu, S. H.; Wang, C. L. Heating-free synthesis of red emissive carbon dots

through separated processes of polymerization and carbonization. *J. Colloid Interface Sci.* **2023**, *646*, 932–939.

[44] Lyu, B.; Li, H. J.; Xue, F. F.; Sai, L.; Gui, B. J.; Qian, D. J.; Wang, X. Y.; Yang, J. H. Facile, gram-scale and eco-friendly synthesis of multi-color graphene quantum dots by thermal-driven advanced oxidation process. *Chem. Eng. J.* **2020**, *388*, 124285.

[45] An, Y. L.; Liu, C.; Chen, M.; Yin, X. J.; Hou, D. F.; Zheng, Y. W.; Shi, R.; He, X. H.; Lin, X. Solid-state carbon dots with tunable fluorescence via surface substitution: Effect of alkyl moieties on fluorescence characteristics. *ACS Sustain. Chem. Eng.* **2023**, *11*, 23–28.

[46] Xia, C. L.; Zhu, S. J.; Feng, T. L.; Yang, M. X.; Yang, B. Evolution and synthesis of carbon dots: From carbon dots to carbonized polymer dots. *Adv. Sci.* **2019**, *6*, 1901316.

[47] Long, P.; Feng, Y. Y.; Cao, C.; Li, Y.; Han, J. K.; Li, S. W.; Peng, C.; Li, Z. Y.; Feng, W. Self-protective room-temperature phosphorescence of fluorine and nitrogen codoped carbon dots. *Adv. Funct. Mater.* **2018**, *28*, 1800791.

[48] Chen, S. W.; Ullah, N.; Wang, T. Q.; Zhang, R. Q. Tuning the optical properties of graphene quantum dots by selective oxidation: A theoretical perspective. *J. Mater. Chem. C* **2018**, *6*, 6875–6883.

[49] Wang, P.; Liu, C.; Tang, W. Q.; Ren, S. X.; Chen, Z. J.; Guo, Y. R.; Rostamian, R.; Zhao, S. L.; Li, J.; Liu, S. X. et al. Molecular glue strategy: Large-scale conversion of clustering-induced emission luminogen to carbon dots. *ACS Appl. Mater. Interfaces* **2019**, *11*, 19301–19307.

[50] Han, Q. R.; Xu, W. J.; Ji, C. Y.; Xiong, G. Y.; Shi, C. S.; Zhang, D. M.; Shi, W. Q.; Jiang, Y. X.; Peng, Z. L. Multicolor and single-component white light-emitting carbon dots from a single precursor for light-emitting diodes. *ACS Appl. Nano Mater.* **2022**, *5*, 15914–15924.